

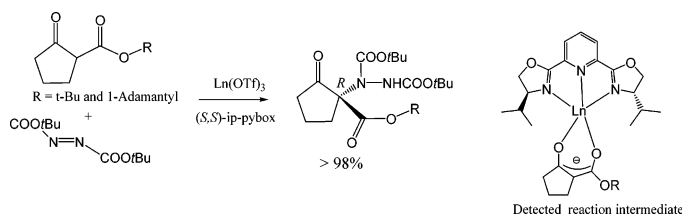
Highly Enantioselective Electrophilic Amination and Michael Addition of Cyclic β -Ketoesters Induced by Lanthanides and (*S,S*)-ip-pybox: The Mechanism[†]

Josep Comelles,[†] Àlex Pericas,[†] Marcial Moreno-Mañas,[‡] Adelina Vallribera,^{†,*}
Galí Drudis-Solé,[†] Agusti Lledos,[†] Teodor Parella,[†] Anna Roglans,[§]
Santiago García-Granda,^{||} and Laura Rocés-Fernández^{||}

Department of Chemistry, Universitat Autònoma de Barcelona, Cerdanyola, 08193-Barcelona, Spain,
Department of Chemistry, Universitat de Girona, 17071-Girona, Spain, and Departamento de Química
Física y Analítica, Universidad de Oviedo, Julián Clavería 8, 33006-Oviedo, Spain

adelina.vallribera@uab.es

Received November 2, 2006



High enantioselection is obtained in Michael additions of cyclic β -ketoesters in the presence of lanthanum triflates and (*S,S*)-ip-pybox. Intermediates based on simultaneous coordination of the lanthanide to both (*S,S*)-ip-pybox and β -ketoester (in keto and enolate forms) are detected by means of ESI mass spectrometry and NMR experiments, and a possible mechanism is proposed through theoretical calculations.

2 Introduction

Michael additions to electronically poor C=C and N=N bonds catalyzed by metals have attracted a great deal of attention.¹ The reactions of cyclic ketoesters² with dialkyl azodicarboxylates³ (Scheme 1) are a convenient model to study the enantioselectivity of electrophilic amination due to the rigidity of the nucleophile and the reactivity of the electrophile. Jørgensen reported the reaction of β -ketoesters with dibenzyl azodicarboxylate in the presence of the pair Cu(OTf)₂-(*S*)-Ph-Box/**1a** or Cu(OTf)₂-(*R*)-Ph-Box/**1b**. Yields and enantiomeric excesses (ee) were excellent, and an absolute *R* configuration was assigned to the compound formed from **1a** by analogy with the well-proved configuration of open ketoesters.² Similar results

have been disclosed by Ma.³ The reaction of **1b** with **2** catalyzed by the alkaloid β -isocupreidine gave **3b** of undisclosed absolute configuration in 89% ee.⁴ Also, reactions of **1a** with dibenzyl azodicarboxylate afforded the Michael adducts in 88–90% ee (*R*, under cinchonine catalysis) or 87% ee (*S*, under cinchonidine catalysis).⁵

We have introduced a new chiral inductor of the Box family featuring adamantyl groups (*R,R*)-adam-box. Combined with copper sources, it gave excellent results in cyclopropanations, Diels–Alder reactions, and allylic oxidations.⁶ Then, as we were particularly interested in Michael reactions,^{1b,7} reactions using the combination of Cu(II) and Ni(II) ionic salts with (*R,R*)-

* To whom correspondence should be addressed. Fax: 34 935811254. Tel: 34 935813045.

[†] Dedicated to Prof. Miquel Yus on the occasion of his 60th birthday.

[‡] Universitat Autònoma de Barcelona.

[§] Deceased on February 20, 2006.

^{||} Universitat de Girona.

^{||} Universidad de Oviedo.

(1) For recent reviews, see: (a) Christoffers, J. *Eur. J. Org. Chem.* **1998**, 1259; (b) Comelles, J.; Moreno-Mañas, M.; Vallribera, A. *Arkivoc* **2005** (Part ix), 207.

(2) Marigo, M.; Juhl, K.; Jørgensen, K. A. *Angew. Chem., Int. Ed.* **2003**, *42*, 1367.

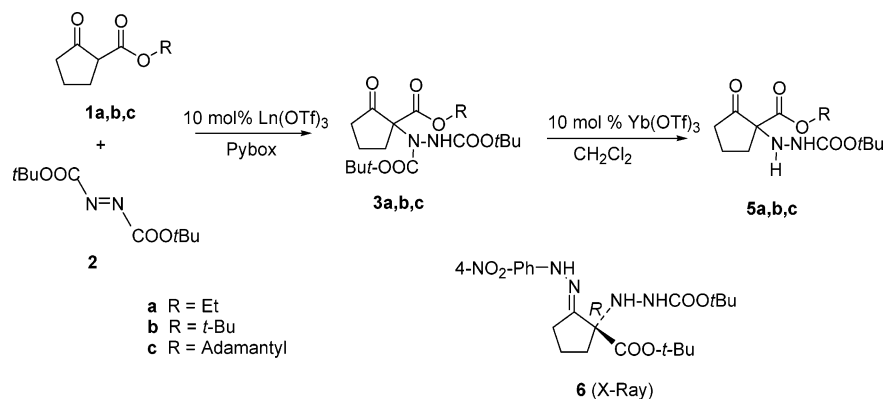
(3) Ma, S.; Jiao, N.; Zheng, Z.; Ma, Z.; Lu, Z.; Ye, L.; Deng, Y.; Chen, G. *Org. Lett.* **2004**, *6*, 2193.

(4) Saaby, S.; Bella, M.; Jørgensen, K. A. *J. Am. Chem. Soc.* **2004**, *126*, 8120.

(5) Pihko, P.M.; Pohjakallio, A. *Synlett* **2004**, 2115.

(6) Clariana, J.; Comelles, J.; Moreno-Mañas, M.; Vallribera, A. *Tetrahedron: Asymmetry* **2002**, *13*, 1551.

(7) (a) Clariana, J.; Gálvez, N.; Marchi, C.; Moreno-Mañas, M.; Vallribera, A.; Molins, E. *Tetrahedron* **1999**, *55*, 7331; (b) Meseguer, M.; Moreno-Mañas, M.; Vallribera, A. *Tetrahedron Lett.* **2000**, *41*, 4093; (c) Marchi, C.; Trepát, E.; Moreno-Mañas, M.; Vallribera, A.; Molins, E. *Tetrahedron* **2002**, *58*, 5699; (d) Martínez, S.; Meseguer, M.; Casas, L.L.; Rodríguez, E.; Molins, E.; Moreno-Mañas, M.; Roig, A.; Sebastián, R. M.; Vallribera, A. *Tetrahedron* **2003**, *59*, 1553; (e) Comelles, J.; Moreno-Mañas, M.; Pérez, E.; Roglans, A.; Sebastián, R. M.; Vallribera, A. *J. Org. Chem.* **2004**, *69*, 6834.

SCHEME 1. Electrophilic Amination of Ketoesters **1a,b,c**

adam-box and commercial (*S,S*)-*t*-Bu-Box were tested, negligible enantiomeric excesses being obtained in all cases.^{7c} Moreover, very preliminary results showed that the combination of Cu(OTf)₂ and commercially available (*S,S*)-*ip*-pybox, **4a**, (Figure 1) for the reaction of ketoester **1b** with **2** gave a maximum of 30% ee. On the other hand, the versatility offered by lanthanides and their increased coordination numbers⁸ suggested to us that we should test the combination of (*R,R*)-adam-pybox, **4b**,⁹ or (*S,S*)-*ip*-pybox, **4a**, (Figure 1) and lanthanides in the Michael reaction, whose catalysis by metals has interested us for some time.

Even though the mechanism for some Michael additions is well studied,^{10a–e} and we have previously reported a mechanism study on the reaction of Cu(II)-based catalysts,^{7c} no such study has been carried out for Michael additions where the catalyst is a derivative of a lanthanide. To cast some light on the mechanism and to identify the intermediates, ESI-MS and NMR experiments have been carried out. The information of the intermediates present proved highly valuable and eased the study of the mechanism through computational means. This not only revealed a possible mechanism for Michael additions catalyzed by lanthanides but also revealed the role the lanthanide is playing as a catalyst.

Results and Discussion

Preparative Work. Our initial results are in Table 1. We soon noticed that (*S,S*)-*ip*-pybox, **4a**, gave better results than its adamantyl congener **4b** in terms of ee's when using the ethyl ketoester **1a** (entries 1–6). Absolute configurations were assigned by comparison with ref 2.

Next, we explored the effect of the size of the ester group in **1**. In general, the *t*-butyl ketoester **1b** (entries 7–14) and adamantyl ketoester **1c** (entries 15–16) gave better results than ethyl ester **1a**, and within this series the best results were

obtained with **1b** and europium (entries 10 and 11). The different ee's obtained with different lanthanides are influenced by the different coordination ability as well as by the different ionic radii. Whereas scandium triflate was inactive even from the viewpoint of the chemical yield, larger ions such as europium and lanthanum gave interesting results with both **4a** and **4b** as pyboxes. Thus, a conservative figure of >95% ee was secured with **1b**, europium triflate, and pybox **4a**. We had observed in preliminary results that the absence of water was essential to obtain good reactivity and high ee's (compare entries 10 and 11), and consequently, all reactions were performed in the presence of 4 Å molecular sieves. Compound **1c** was prepared in 69% yield by a modification of a general transesterification method¹¹ from a mixture of ketoester **1a**, 1-adamantanol, and zinc oxide (see Supporting Information).

Then, we studied the influence of solvent polarity on the reaction of 1-adamantyl ketoester **1c** with **2** (Scheme 2). Synthetically useful yields were secured in all tested solvents, the dependence of ee on solvent polarity being clear, the more polar common solvents giving the best results (Table 2). Thus, reaction in acetonitrile gave 100% ee in the presence of 0.1% of catalyst (entry 5, Table 2).

Prolonged treatment of **3** with ytterbium triflate in dichloromethane resulted in regioselective de-*tert*-butoxycarbonylation to afford **5** (Schemes 1 and 2). This permitted a simpler analysis of enantiomeric excesses by ¹H NMR using a chiral shift reagent, which was not possible on compounds **3**. Moreover, it facilitated the determination of the *R* absolute configuration of **5b** in the form of 4-nitrophenylhydrazone, **6** (Scheme 1).

The advantage of using adamantyl esters is that the adamantyl group confers crystallinity, and consequently, the absolute configuration of **3c** can be directly determined by X-ray diffraction analysis. The configurations of **3a** were assigned by analogy with **3b,c**, assuming that the same major enantiomer was obtained in all cases under identical conditions.

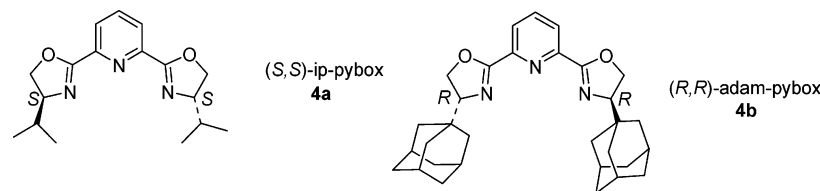
Finally, we studied the reactions of **1b,c** with butenone **7** (Scheme 3 and Table 3). First, the reaction of ketoesters **1b,c** permitted us to identify ytterbium as the lanthanide of choice in this particular case (entries 1–3, Table 3) using ligand **4a**. On the other hand, europium was the best lanthanide when using **2** with the same ketoesters **1b,c**; thus, the Michael acceptor plays a fundamental role in the choice of the metal ion. The determination of enantiomeric composition of chiral **8b** was done through NMR analysis by two different methods: by

(8) Mikami, K.; Terada, M.; Matsuzawa, H. *Angew. Chem., Int. Ed.* **2002**, *41*, 3554.

(9) For a recent review on pyridine-2,6-bis(oxazolines) (pybox's) see: (a) Desimoni, G.; Faita, G.; Quadrelli, P. *Chem. Rev.* **2003**, *103*, 3119. For a recent reviews on oxazoline-containing ligands see: (b) McManus, H. A.; Guiry, P. *Chem. Rev.* **2004**, *104*, 4151; (c) Desimoni, G.; Faita, G.; Jørgensen, K. A. *Chem. Rev.* **2006**, *9*, 3561.

(10) (a) Hayashi, T.; Takahashi, M.; Takaya, Y.; Ogasawara, M.; *J. Am. Chem. Soc.* **2002**, *124*, 5052; (b) Okumoto, S.; Yamabe, S. *J. Org. Chem.* **2000**, *65*, 1544; (c) Yasuda, M.; Chiba, K.; Ohigashi, N.; Katoh, Y.; Baba, A. *J. Am. Chem. Soc.* **2003**, *125*, 7291; (d) Castelli, V.; Cort, A.; Mandolini, L.; Reinhoudt, D.; Schiaffino, L. *Eur. J. Org. Chem.* **2003**, 627; (e) Chatfield, D.; Augsten, A.; D'Chuna, C.; Lewandowska, E.; Wnuk, S. *Eur. J. Org. Chem.* **2004**, 313.

(11) Bandgar, V.S.; Sadararte, V. S.; Uppala, L.S. *J. Chem. Res.* **2001**, 16.

FIGURE 1. Formulas of pyboxes **4a** and **4b**.TABLE 1. Electrophilic Amination of **1a,b,c** (Scheme 1)^{a,b}

entry	Ln ⁺³	ionic radii (Å), Ln ⁺³	pybox	1	temp (°C)	yield of 3 (%)	ee ^{b,c} (%)
1	Yb ⁺³	0.985	4a	1a	r. t.	3a , 85	68 (<i>R</i>)
2	Yb ⁺³	0.985	4b	1a	r. t.	3a , 74	0
3	Eu ⁺³	1.066	4a	1a	0	3a , 82	62 (<i>R</i>)
4	Eu ⁺³	1.066	4b	1a	0	3a , 88	12 (<i>S</i>)
5	La ⁺³	1.160	4a	1a	0	3a , 84	52 (<i>R</i>)
6	La ⁺³	1.160	4b	1a	0	3a , 79	18 (<i>R</i>)
7	Sc ⁺³	0.870	4a	1b	r. t.	3b , 0	–
8	Yb ⁺³	0.985	4a	1b	–41 → 0 ^d	3b , 70	70 (<i>R</i>)
9	Yb ⁺³	0.985	4b	1b	r. t.	3b , 31	66 (<i>S</i>)
10	Eu ⁺³	1.066	4a	1b	r. t.	3b , 55	67 (<i>R</i>) ^e
11	Eu ⁺³	1.066	4a	1b	–41 → 0 ^d	3b , 81	>95 (<i>R</i>) ^f
12	Eu ⁺³	1.066	4b	1b	–41	3b , 66	86 (<i>S</i>)
13	La ⁺³	1.160	4a	1b	0	3b , 78	22 (<i>S</i>)
14	La ⁺³	1.160	4b	1b	–41	3b , 71	84 (<i>S</i>)
15	Yb ⁺³	0.985	4a	1c	0	3c , 62	55 (<i>R</i>)
16	Eu ⁺³	1.066	4a	1c	0	3c , 85	71 (<i>R</i>)

^a Reactions performed in dichloromethane. ^b ee determined by ¹H NMR by adding the chiral shift reagent Eu(hfc)₃ on **5a,b**. ^c Absolute configuration of **3b** was determined by X-ray diffraction analysis of its derivative **6**; absolute configuration of **3a** was assigned by analogy and was coherent to ref 2. ^d Three hours at –41 °C and then 2 h more at 0 °C. ^e Reaction performed in not dried CH₂Cl₂ and without 4 Å molecular sieves. ^f [α]^D = +11.3 (*c* = 1.6, CH₂Cl₂).

adding the chiral shift reagent Eu(hfc)₃ and by addition of (*R,R*)- α,α -bis(trifluoromethyl)-9,10-anthracenedimethanol ((*R,R*)-ABTE),¹² a chiral solvating agent useful for enantiomeric resolution of β -dicarbonyl compounds.¹³ Then, we studied the behavior of ytterbium triflate in the reaction of **1c** with **7** in acetonitrile at different temperatures (entries 4–7). We noticed that at –41 °C the ee was as high as 96%, the highest ever obtained in the reaction of **1** with **7**.

The assignment of *R* as the absolute configuration of **8b,c**, which provisionally we accept, deserves some comments. Our compound **8b** (*t*-Bu ester, Entry 1, Table 3) showed a positive specific rotation as for the same compound prepared by Sodeoka ([α]^D = +8.7 (*c* = 0.41, CHCl₃), 92% ee).¹⁴ The assignment of Sodeoka was based on the conversion of **8b** into the methyl ester ([α]^D = –12.4 (*c* = 0.44, CHCl₃), featuring a negative value of specific rotation as it was described previously by Christoffers ([α]^D = –5.6 (*c* = 9.9, CHCl₃), 31% ee).¹⁵ Finally, this last assignment relies upon an assignment based on the CD exciton chirality method.¹⁶ We assume that the same configuration is favored for **8b** and **8c**.

(12) Pomares, M.; Sánchez-Ferrando, F.; Virgili, A.; Alvarez-Larena, A.; Piniella, J. F. *J. Org. Chem.* **2002**, *67*, 753.

(13) Comelles, J.; Estivill, C.; Moreno-Mañanas, M.; Virgili, A.; Vallribera, A. *Tetrahedron*, **2004**, *60*, 11541.

(14) (a) Hamashima, Y.; Hotta, D.; Sodeoka, M. *J. Am. Chem. Soc.* **2002**, *124*, 11240; (b) Hamashima, Y.; Takano, H.; Hotta, D.; Sodeoka, M. *Org. Lett.* **2003**, *5*, 3225; (c) Hamashima, Y.; Hotta, D.; Natsuko, U.; Tsuchiya, Y.; Suzuki, T.; Sodeoka, M. *Adv. Synth. Catal.* **2005**, *347*, 1576.

(15) Christoffers, J.; Röbber, U.; Werner, T. *Eur. J. Org. Chem.* **2000**, 701.

(16) Tamai, Y.; Kamifuku, A.; Koshiishi, E.; Mayano, S. *Chem. Lett.* **1995**, 957.

The Mechanism. Mechanistic aspects are crucial for the better understanding of selectivity aspects of these lanthanide-catalyzed Michael reactions. We have studied in depth the mechanism of Michael additions with copper-based ionic catalysts (Cu(SbF₆)₂ and (*R,R*)-adam-box) or covalent (copper(II)salicylaldehyde), and they have a common feature: the intermediacy of copper(II) enolates such as **9a,b** (Figure 2, detected by ESI-MS).^{7e} Lanthanides have increased coordination numbers, which makes them ideal for simultaneous coordination of both reaction partners as well as ancillary chiral ligands around the metal. Shibasaki et al. found ESI-MS evidence for the simultaneous coordination of the chiral ligand (BINOL derivatives) and the ketoester in the form of enolate.¹⁷

Intermediates Detected by ESI Mass Spectrometry. To obtain new insights to the mechanism we conducted an ESI mass spectrometry study to detect short-lived reaction intermediates present in the solution. The electrospray ionization mass spectrometry (ESI-MS)¹⁸ is a technique that has become increasingly popular as a mechanistic tool for studying transient intermediates involved in organometallic catalytic reactions.¹⁹

Our investigation was based on the reaction of 1-adamantyl ketoester **1c** with two different electrophiles, the azodicarboxylate **2** and butenone **7**, using La(OTf)₃/(*S,S*)-ip-pybox as a catalytic system in acetonitrile at room temperature. Lanthanum was selected in ESI studies to allow comparison with the NMR experiments that will be explained below. First of all, individual components of the reaction were analyzed as well as mixtures of two or more components (see supplementary data for ESI mass spectra of entries 1–14 in Table 4). Finally, the ongoing reaction was also injected into the mass spectrometer (entry 15 in Table 4 and Figure 3).

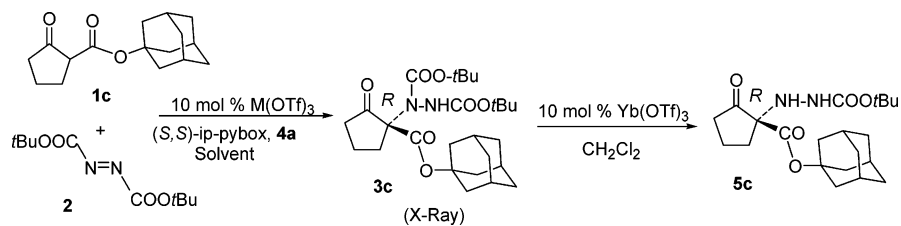
Pure Products. To identify every possible compound in the mass spectra of subsequent mixtures, starting material **1c**, ligand pybox **4a**, lanthanum salt La(OTf)₃, and final products **3c** and **8c** were analyzed by ESI mass spectrometry. The results are summarized in Table 4 (entries 1–5). In all cases, the molecular ion [M + H]⁺ together with solvent and/or cation adducts could be clearly observed.

Binary Mixtures. The ESI-MS spectrum of a stoichiometric mixture of pybox **4a** and La(OTf)₃ (Entry 6) showed three

(17) Majima, K.; Takita, R.; Okada, A.; Ohshima, T.; Shibasaki, M. *J. Am. Chem. Soc.* **2003**, *125*, 15837.

(18) For a monograph on ESI-MS, see: Cole, R. B. *Electrospray Ionization Mass Spectrometry, Fundamentals, Instrumentation and Applications*; Wiley: New York, 1997.

(19) For a recent review about investigation of chemical reactions using this technique, see the following review and references cited therein: (a) Santos, L. S.; Knaack, L.; Metzger, J. O. *Int. J. Mass Spectrom.* **2005**, *246*, 84. For the application of ESI-MS to inorganic and organometallic chemistry, see the following reviews and references cited therein: (b) Colton, R.; D'Agostino, A.; Traeger, J. C. *Mass Spectrom. Rev.* **1995**, *14*, 79; (c) Henderson, W.; Nicholson, B. K.; McCaffrey, L. J. *Polyhedron* **1998**, *17*, 4291. (d) Traeger, J. C. *Int. J. Mass Spectrom.* **2000**, *200*, 387; (e) Plattner, D. A. *Int. J. Mass Spectrom.* **2001**, *207*, 125; (f) Plattner, D. A. *Top. Curr. Chem.* **2003**, *225*, 153; (g) Chen, P. *Angew. Chem., Int. Ed.* **2003**, *42*, 2832; (h) Evans, W. J.; Johnston, M. A.; Fujimoto, Cy, H.; Greaves, J. *Organometallics* **2000**, *19*, 4258.

SCHEME 2. Reaction of Ketoester **1c**

peaks: (i) $m/z = 738$ corresponding to a complex of lanthanum with one pybox ligand [(pybox)La(OTf)₂]⁺; (ii) $m/z = 779$ corresponding to the same intermediate as before but coordinated with one molecule of acetonitrile solvent [(pybox)La(OTf)₂CH₃CN]⁺; and (iii) $m/z = 1039$ consistent with a lanthanum complex coordinated to two pybox ligands [(pybox)₂La(OTf)₂]⁺.

Stoichiometric mixtures of La(OTf)₃ with ketoester **1c** or the final products **3c** and **8c** were injected into the mass spectrometer to see if there was any interaction of lanthanum with the compounds in the absence of pybox ligand. In all three cases, species corresponding to the lanthanum coordinated to two molecules of ketoester **1c** ($m/z = 961$, [La(**1c**)₂(OTf)₂]⁺) (entry 7), of final product **3c** ($m/z = 1421$, [La(**3c**)₂(OTf)₂]⁺) (entry 8), and final product **8c** ($m/z = 1101$, [La(**8c**)₂(OTf)₂]⁺) (entry 9) were clearly observed.

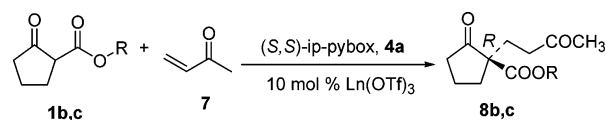
Ternary and Quaternary Mixtures. When ketoester **1c** was added to a previously formed mixture of La(OTf)₃ and pybox **4a** in a molar ratio of 1:0.4:0.4, the ESI mass spectrum showed a variety of signals (entry 10 in Table 4): (i) two peaks at $m/z = 850$ and 1151 , agreeing with the in situ formation of lanthanum enolate with one pybox ligand [(pybox)La(enolate-**1c**)OTf]⁺ or two pybox ligands [(pybox)₂La(enolate-**1c**)OTf]⁺, respectively; (ii) a peak centered at $m/z = 1000$, corresponding to an intermediate where the neutral ketoester **1c** coordinates the lanthanum atom [(pybox)La(**1c**)(OTf)₂]⁺; (iii) the peak at $m/z = 1039$, corresponding to [(pybox)₂La(OTf)₂]⁺.

The two electrophilic starting compounds, **2** and **7**, were separately added to a previously formed mixture of La(OTf)₃ and pybox **4a**, but only the three peaks observed in entry 6 corresponding to species in which the lanthanum is coordinated to the pybox ligand were detected. No peaks corresponding to species where lanthanum was coordinated either to **2** or **7** were observed. On the other hand, when the two final products, **3c** and **8c**, were added separately to a mixture of La(OTf)₃ and pybox ligand, peaks consistent with [(pybox)La(**3c** or **8c**)(OTf)₂]⁺ at $m/z = 1230$ (for **3c**) (entry 11) and $m/z = 1070$ (for **8c**) (entry 12) were clearly observed.

TABLE 2. Dependence of ee of **3c** on Solvent Polarity (Scheme 2)

entry	Ln ³⁺	solvent	temp (°C)	ε	E _T ^N	ee (%) ^a
1	La ³⁺	CH ₃ CN	25	35.94	0.460	89 (R)
2	Eu ³⁺	CH ₃ CN	25	35.94	0.460	93 (R)
3	Eu ³⁺	CH ₃ CN	0	35.94	0.460	95 (R)
4	Eu ³⁺	CH ₃ CN	-41	35.94	0.460	98 (R)
5	Eu ³⁺	CH ₃ CN	-41	35.94	0.460	100 ^{b,c} (R)
6	Eu ³⁺	ClCH ₂ CH ₂ Cl	0	10.36	0.327	73 (R)
7	Yb ³⁺	CH ₂ Cl ₂	0	8.93	0.309	55 (R)
8	Eu ³⁺	CH ₂ Cl ₂	0	8.93	0.309	71 (R)
9	Eu ³⁺	DME	0	7.20	0.231	30 (R)
10	Eu ³⁺	THF	0	7.58	0.207	50 (R)
11	Eu ³⁺	cyclohexane	0	2.02	0.006	0

^a ee's determined on **3c** by HPLC; R Configuration determined by X-ray diffraction analysis. ^b [α]_D²⁵ = +7.46 (c = 3.27, CH₂Cl₂). ^c 0.1% of Eu(OTf)₃.

SCHEME 3. Reactions of **1b,c** with Butenone, **7**

The addition of either azodicarboxylate **2** and butenone **7** to the previously formed mixture (La(OTf)₃ + pybox + **1c**) revealed final products **3c** and **8c** coordinated to lanthanum and a pybox ligand (entries 13 and 14). The peaks at $m/z = 1039$ and 1151 are persistent in the two former mass spectrum. The peak at 1151 is in agreement with the in situ formation of lanthanum enolate with two pybox ligands [(pybox)₂La(enolate-**1c**)OTf]⁺. The peaks at $m/z = 1230$ (entry 13) and $m/z = 1070$ (entry 14) could also be assigned to two different species where the lanthanum atom was coordinated to pybox, to ketoester **1c**, and to the corresponding Michael acceptors, **2** and **7**, respectively. However, because the two peaks (1230 and 1070) were observed in the previous ternary mixtures of pybox, La(OTf)₃, and **3c** (entry 11) and pybox, La(OTf)₃, and **8c** (entry 12) and no species were detected when starting materials **2** or **7** were added to a mixture of pybox and La(OTf)₃, we postulate that the two species formed are those where the lanthanum atom is coordinated to the final products.

Ongoing Reaction. In our last set of experiments, we performed the reaction with all the components using 5 molar % of catalyst [**1c** (1 equiv) + **7** (1 equiv) + pybox/La(OTf)₃ (5 molar %)] (entry 15). Samples were taken at different intervals until TLC indicated completion of the reaction. The ESI-MS spectra afforded the signals already observed in entries 10 and 14. Furthermore, a new peak at $m/z = 1031$ appeared, corresponding to lanthanum coordinated to starting material **1c** and final product **8c**. However, it is important to note that lanthanum species containing enolate-**1c** and **1c** disappeared as the reaction ended and the peak corresponding to the lanthanum complex with the final product **8c** started to emerge. At the end of the reaction, only this peak remained.

NMR Spectroscopy. The reaction mechanism was also studied by NMR spectroscopy using different deuterated solvents (chloroform, acetonitrile, and acetone) to detect and confirm possible intermediates and final products as observed by ESI-MS. For this purpose, conventional ¹H, 2D NOESY and diffusion/DOSY²⁰ experiments were recorded at 298 K in several stages (see Supporting Information for the figures of all the recorded NMR spectra). First, a NMR analysis of the starting ligand pybox, **4a**, and the 1-adamantyl ketoester, **1c**, derivatives was made, and their self-diffusion coefficients were in agreement with their relative small volume. Then, as a general trend and independently of the solvent used, the addition of

(20) (a) Johnson, C. S. *Prog. NMR. Spectrosc.* **1999**, *34*, 203; (b) Pregosin, P. S.; Anil, Kumar, P. G.; Fernandez, I. *Chem. Rev.* **2005**, *105*, 2977.

TABLE 3. Reactions of **1b,c** with Butenone **7** (Scheme 3)

entry	Ln ⁺³	1	temp (°C)	solvent	yield of 8 (%)	8 , ee (%) ^a
1	Yb ⁺³	1b	-41 → r. t. ^b	CH ₂ Cl ₂	85	8b , 86 ^{c,d}
2	Eu ⁺³	1b	-41 → r. t. ^b	CH ₂ Cl ₂	81	8b , 65
3	La ⁺³	1b	-41 → r. t. ^b	CH ₂ Cl ₂	81	8b , 0
4	Yb ⁺³	1c	r. t.	CH ₃ CN	44	8c , 80
5	Yb ⁺³	1c	0	CH ₃ CN	64	8c , 84 ^e
6	Yb ⁺³	1c	-20	CH ₃ CN	40	8c , 93
7	Yb ⁺³	1c	-41	CH ₃ CN	96	8c , 96
8	Eu ⁺³	1c	0	CH ₃ CN	62	8c , 59
9	La ⁺³	1c	25	CH ₃ CN	73	8c , 29

^a ee determined by ¹H NMR by two different methods: by adding the chiral shift reagent Eu(hfc)₃ and by addition of a chiral solvating agent ((*R,R*)-ABTE) on **8b**. ee determined by HPLC on **8c**. ^b Six hours at -41 °C an then r.t. ^c Experiment also successful with 1% of Yb(OTf)₃. ^d [α]^D = +2.9 (*c* = 11.0, CH₂Cl₂). ^e [α]^D = +17.4 (*c* = 2.02, CH₂Cl₂).

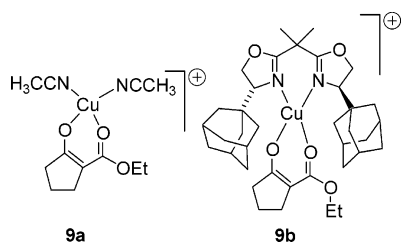


FIGURE 2. Copper enolates detected by ESI-MS in previous studies.

La(OTf)₃ on **4a** induces important changes in the ¹H spectrum. First, considerable downfield chemical shift effects were observed in the range 0.4–0.7 ppm for characteristic pyridinyl and isoxazoline proton chemical shifts of the pybox ligand. In addition, another set of NMR signals showing broader lineshapes are also clearly visible for a second compound. The ratio between these two La(OTf)₃/(*S,S*)-ip-pybox binding compounds was strongly dependent on the solvent and the temperature and the presence of positive cross-peaks in NOESY spectra confirms the presence of several species under a relatively slow equilibrium exchange process that was also fully confirmed by diffusion measurements. For instance, in CDCl₃ at 298 K, the free **4a** compound presents a *D* value of 0.87 × 10⁻⁹ m²/s

TABLE 4. ESI Mass Spectral Data for Compounds and Mixtures^a

entry	compounds and mixtures	identified species ^b
1	1c	<i>m/z</i> = 263 [M + H] ⁺ , 280 [M + NH ₄] ⁺
2	pybox, 4a	<i>m/z</i> = 302 [M + H] ⁺
3	La(OTf) ₃	<i>m/z</i> = 478, 519, 560, 601 [La(OTf) ₂ (CH ₃ CN) _{<i>n</i>}] ⁺ , where <i>n</i> = 1–4
4	3c	<i>m/z</i> = 493 [M + H] ⁺ , 510 [M + NH ₄] ⁺ , 515 [M + Na] ⁺ ,
5	8c	<i>m/z</i> = 333 [M + H] ⁺ , 355 [M + Na] ⁺ , 371 [M + K] ⁺ , 396 [M + Na + CH ₃ CN] ⁺
6	pybox 4a + La(OTf) ₃	<i>m/z</i> = 738 [(pybox)La(OTf) ₂] ⁺ , 779 [(pybox)La(OTf) ₂ CH ₃ CN] ⁺ , 1039 [(pybox) ₂ La(OTf) ₂] ⁺
7	1c + La(OTf) ₃	<i>m/z</i> = 961 [La(1c) ₂ (OTf) ₂] ⁺ , 1002 [La(1c) ₂ (OTf) ₂ CH ₃ CN] ⁺
8	3c + La(OTf) ₃	<i>m/z</i> = 1421 [La(3c) ₂ (OTf) ₂] ⁺
9	8c + La(OTf) ₃	<i>m/z</i> = 1101 [La(8c) ₂ (OTf) ₂] ⁺
10	pybox 4a + La(OTf) ₃ + 1c	<i>m/z</i> = 850 [(pybox)La(enolate- 1c)OTf] ⁺ , 1000 [(pybox)La(1c)(OTf) ₂] ⁺ , 1039 [(pybox) ₂ La(OTf) ₂] ⁺ , 1151 [(pybox) ₂ La(enolate- 1c)OTf] ⁺
11	pybox 4a + La(OTf) ₃ + 3c	<i>m/z</i> = 1039 [(pybox) ₂ La(OTf) ₂] ⁺ , 1230 [(pybox)La(3c)(OTf) ₂] ⁺ , 1421 [La(3c) ₂ (OTf) ₂] ⁺
12	pybox 4a + La(OTf) ₃ + 8c	<i>m/z</i> = 1039 [(pybox) ₂ La(OTf) ₂] ⁺ , 1070 [(pybox)La(8c)(OTf) ₂] ⁺ , 1101 [La(8c) ₂ (OTf) ₂] ⁺
13	pybox 4a + La(OTf) ₃ + 1c + 2	<i>m/z</i> = 1039 [(pybox) ₂ La(OTf) ₂] ⁺ , 1151 [(pybox) ₂ La(enolate- 1c)OTf] ⁺ , 1230 [(pybox)La(3c)(OTf) ₂] ⁺
14	pybox 4a + La(OTf) ₃ + 1c + 7	<i>m/z</i> = 1039 [(pybox) ₂ La(OTf) ₂] ⁺ , 1070 [(pybox)La(8c)(OTf) ₂] ⁺ , 1101 [La(8c) ₂ (OTf) ₂] ⁺ , 1151 [(pybox) ₂ La(enolate- 1c)OTf] ⁺
15	Ongoing reaction: 1c + 7 + pybox + La(OTf) ₃	5 min: <i>m/z</i> = 850 [(pybox)La(enolate- 1c)OTf] ⁺ (Major), 1000 [(pybox)La(1c)(OTf) ₂] ⁺ , 1031 [La(1c)(8c)(OTf) ₂] ⁺ 10 min: <i>m/z</i> = 850 [(pybox)La(enolate- 1c)OTf] ⁺ , 1000 [(pybox)La(1c)(OTf) ₂] ⁺ , 1031 [La(1c)(8c)(OTf) ₂] ⁺ , 1070 [(pybox)La(8c)(OTf) ₂] ⁺ , 1101 [La(8c) ₂ (OTf) ₂] ⁺ 20 min: 1070 [(pybox)La(8c)(OTf) ₂] ⁺ , 1101 [La(8c) ₂ (OTf) ₂] ⁺

^a All ESI-MS analyses were performed with samples dissolved in CH₃CN. The HPLC mobile phase was a 70:30 mixture of CH₃CN and H₂O. ^b Unidentified ions in the spectra have not been included.

whereas these two different set of NMR signals in the complex mixture present *D* values of 0.43 × 10⁻⁹ m²/s and 0.36 × 10⁻⁹ m²/s, respectively, which are in strong agreement with the presence of higher molecular-mass complexes of the type [(pybox)La(OTf)₂]⁺ and [(pybox)₂La(OTf)₂]⁺ as observed by ESI mass spectrometry. Similar results were also obtained in acetone and acetonitrile.

Interesting changes in the ¹H NMR spectrum were also observed when adding a racemic mixture of (*R*)- and (*S*)-dicarbonylic **1c** compound on the chiral La(OTf)₃/(*S,S*)-ip-pybox complex. First of all, the resulting broad unresolved resonances evidence for important dynamic processes between several complexed species in solution, as confirmed by variable-temperature ¹H spectra. Second, two different triplets in a 1:1 ratio appear around 3.2–3.4 ppm corresponding to the methylene α -dicarbonylic protons of the two different diastereoisomeric forms of the ternary [(pybox)La(**1c**)(OTf)₂]⁺ complex. In contrast to the free form of **1c**, these two triplets show positive exchange cross-peaks in the NOESY spectrum with the residual hydroxyl labile protons resonating as a broad signal near to 5.0 ppm, confirming the presence of tautomeric keto–enol equilibria. Finally, whereas the signals belonging to the pybox ligand in the ternary complex present similar *D* values as the monoligand [(pybox)La(OTf)₂]⁺ specie 0.44 × 10⁻⁹ m²/s, the signals of 3.3 and 3.4 ppm belonging to the intercarbonylic proton of **1c** in the diastereoisomeric complex [(pybox)La(**1c**)(OTf)₂]⁺ compounds present a *D* value of 0.85 × 10⁻⁹ m²/s and 0.76 × 10⁻⁹ m²/s. These values are different to the free **1c** compound 1.14 × 10⁻⁹ m²/s confirming the presence of a relatively slow complex equilibrium between the free form of **1c** and the two diastereoisomeric [(pybox)La(**1c**)(OTf)₂]⁺ forms, both also under the effect of keto–enol equilibria. The different *D* values for diastereoisomeric [(pybox)La(**1c**)(OTf)₂]⁺ forms also accounts for their different association affinity to the La complex. The final evidence for the presence of the ternary [(pybox)La-(**1c**)(OTf)₂]⁺ complex is the weak but very important interligand NOE observed between the aliphatic adamantyl

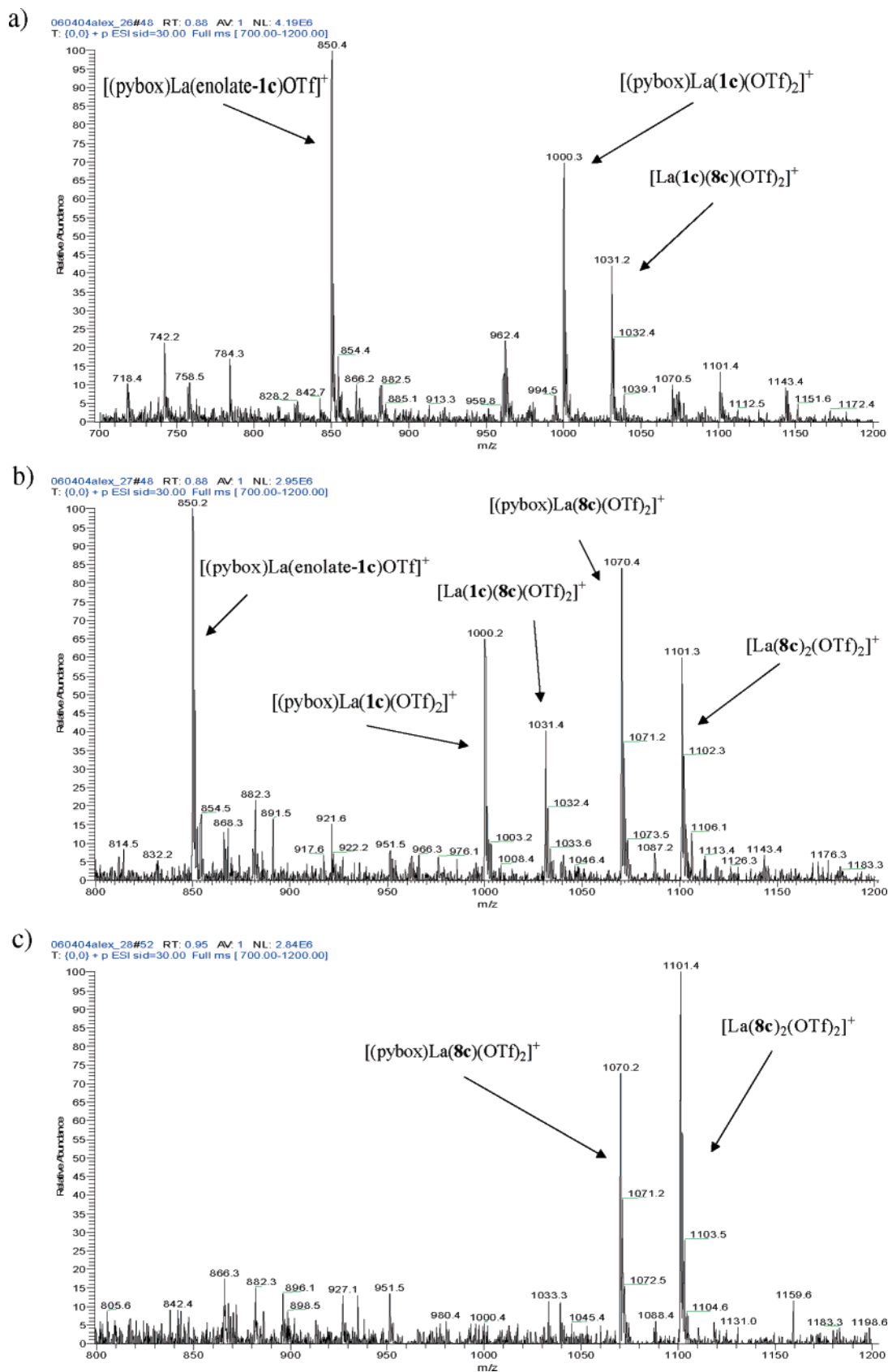


FIGURE 3. ESI(+)-MS of a mixture of ketoester **1c**, butenone **7**, pybox, and La(OTf)₃ after mixing for: (a) 5 min; (b) 10 min; and (c) 20 min.

protons of the **1c** moiety and the methyl protons of the pybox ligand. All mentioned NMR spectra are provide in the Supporting Information.

Discussion of ESI-MS and NMR Spectroscopy Results. Two different series of important species have been detected by ESI-MS experiments: intermediates with neutral coordination

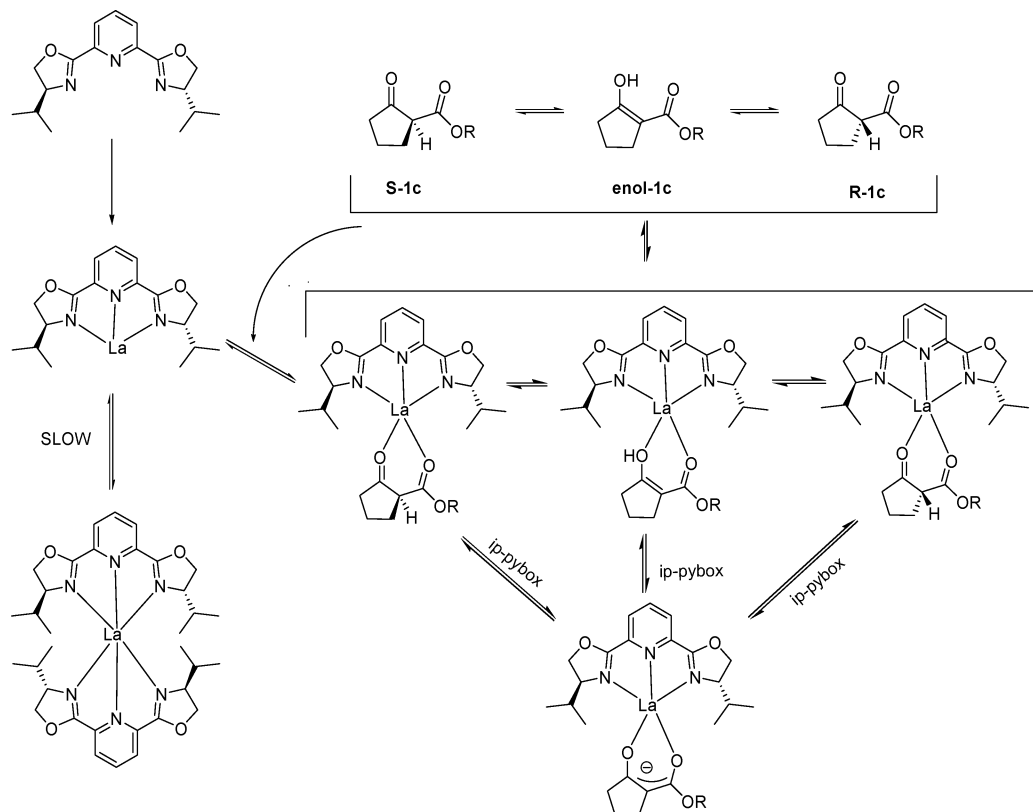


FIGURE 4. Species and equilibria proposed from NMR experiments.

of ketoester **1c** ($[(\text{pybox})\text{La}(\mathbf{1c})(\text{OTf})_2]^+$) and intermediates with coordination through the ketoester enolate-**1c** ($[(\text{pybox})\text{La}(\text{enolate-1c})\text{OTf}]^+$ and $[(\text{pybox})_2\text{La}(\text{enolate-1c})\text{OTf}]^+$). Moreover, both species containing **1c** and enolate-**1c** disappeared in the ongoing reaction experiments. NMR experiments clearly support the existence of ternary complexes where the dicarbonyl moiety is under keto–enol equilibrium. Thus, in the presence of a base (ip-pybox) the enolate can be easily formed (Figure 4). Furthermore, all Michael reactions described in this manuscript have been previously carried out in a racemic version (in the absence of chiral box ligand) using $\text{Ln}(\text{OTf})_3$ as catalyst. In these conditions, conjugate additions were slower than the ones carried out in the presence of the chiral box ligand. For example, 16 h were needed to complete the reaction of **1c** and **2** at room temperature in the presence of 10% of $\text{Eu}(\text{OTf})_3$, whereas when adding the chiral pybox, the same reaction is finished in 2 h at -41°C . Consequently, the chiral box ligand has a catalytic effect probably acting as a base extracting the acidic intercarbonylic proton of Michael donors **1**, acting as a bifunctional chiral ligand.²¹ In fact, we have proved that the racemic reaction of **1c** and **2** is slowly catalyzed (10 h) by ip-pybox (15 mol %) at room temperature. This supports the coordination through the enolate as intermediate of this lanthanides-catalyzed Michael reaction.

Theoretical Calculations. The detection of the intermediates of the reaction by ESI mass spectrometry and NMR experiments has eased the study of the mechanism through theoretical calculations. The relative energies of each of the intermediates can be obtained by computational methods and so can the energies of the transition state, which provides us with quantita-

tive data to discern possible from impossible mechanisms. The knowledge of the mechanism should also provide us with enough data to describe the role the metallic center is playing in the reaction.

All calculations have been performed with the B3LYP DFT functional as implemented in the Gaussian98²² package. The quasi-relativistic MWB large-core pseudopotential was used for lanthanum,²³ together with the MWB basis set. The rest of the atoms were described by the 6-31g basis set if the atom is never attached to lanthanum and by the 6-31g* basis set if it is at any point in the mechanism (N and Cl atoms and carbonyl oxygens). In all the intermediates involving the metal, the triflate anions were replaced by chloride anions, whereas the possible organic substituents at the ester position of the ketoester were replaced by a methyl. A smaller model of the real catalyst, as shown in Figures 5–8, was used.

(22) Frisch, M. J.; Trucks, G. W.; Schlegel, H. B.; Scuseria, G. E.; Robb, M. A.; Cheeseman, J. R.; Zakrzewski, V. G.; Montgomery, J. A., Jr.; Stratmann, R. E.; Burant, J. C.; Dapprich, S.; Millam, J. M.; Daniels, A. D.; Kudin, K. N.; Strain, M. C.; Farkas, O.; Tomasi, J.; Barone, V.; Cossi, M.; Cammi, R.; Mennucci, B.; Pomelli, C.; Adamo, C.; Clifford, S.; Ochterski, J.; Petersson, G. A.; Ayala, P. Y.; Cui, Q.; Morokuma, K.; Malick, D. K.; Rabuck, A. D.; Raghavachari, K.; Foresman, J. B.; Cioslowski, J.; Ortiz, J. V.; Stefanov, B. B.; Liu, G.; Liashenko, A.; Piskorz, P.; Komaromi, I.; Gomperts, R.; Martin, R. L.; Fox, D. J.; Keith, T.; Al-Laham, M. A.; Peng, C. Y.; Nanayakkara, A.; Gonzalez, C.; Challacombe, M.; Gill, P. M. W.; Johnson, B. G.; Chen, W.; Wong, M. W.; Andres, J. L.; Head-Gordon, M.; Replogle, E. S.; Pople, J. A. *Gaussian 98*, revision A.11; Gaussian, Inc.: Pittsburgh, PA, 2001.

(23) (a) Maron, L.; Eisenstein, O. *J. Phys. Chem. A* **2000**, *104*, 7140; (b) Eisenstein, O.; Maron, L.; *J. Organomet. Chem.* **2002**, *647*, 190; (c) Barros, N.; Eisenstein, O.; Maron, L. *J. Chem. Soc., Dalton Trans.* **2006**, 25, 3052; (d) Maron, L.; Werkema, E. L.; Perrin, L.; Eisenstein, O.; Andersen, R. A. *J. Am. Chem. Soc.* **2005**, *127*, 279; (e) Werkema, E. L.; Messines, E.; Perrin, L.; Maron, L.; Eisenstein, O.; Andersen, R. A. *J. Am. Chem. Soc.* **2005**, *127*, 7781.

(21) Corey, E. J.; Wang, Z. *Tetrahedron Lett.* **1993**, *34*, 4001.

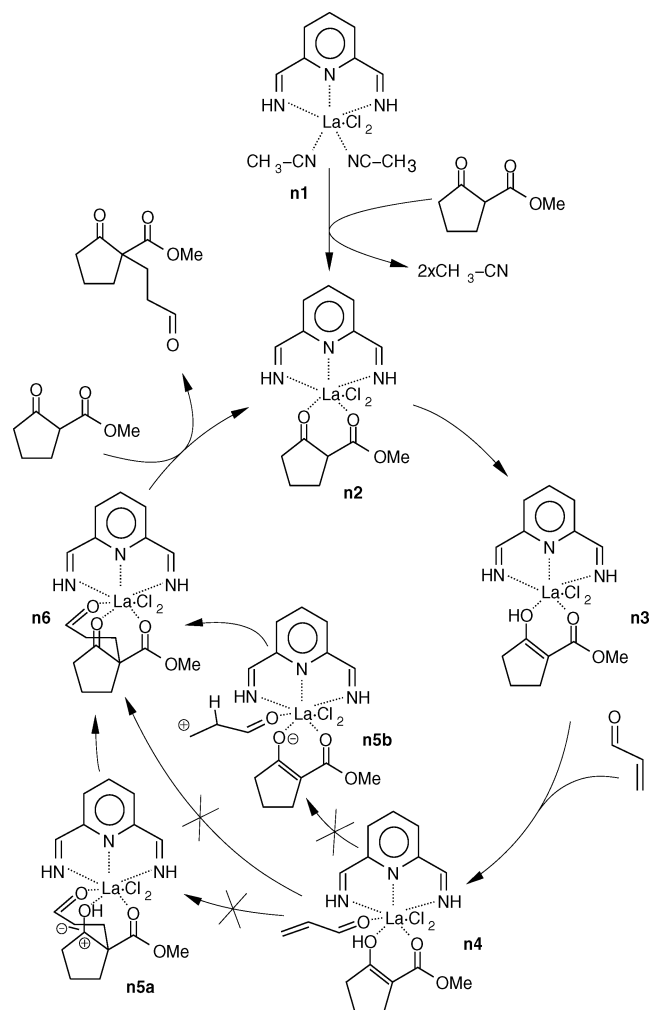


FIGURE 5. Catalytic cycle for the neutral pathway. All the species involving the lanthanum have a +1 charge.

Neutral Mechanism. The first catalytic cycle studied evolves through the dicarbonyl and enol forms of the ketoester, and will thereafter be referred as the neutral mechanism. The catalytic

cycle for this mechanism is depicted in Figure 5. The first step involves the replacement of the two solvent molecules bound to the metal in **n1** by the ketoester. The next two steps can be carried in any order and imply the conversion of the ketoester from the keto to the enol form (**n3**) and the coordination of the second reactant, the Michael acceptor, to give molecule **n4**. Intermediate **n2** (or **n3**) was observed in the ESI-MS experiments ($m/z = 1000$ [(pybox)La(**1c**)(OTf)₂]⁺). The crucial step comes next and involves the formation of the new C–C bond and the transfer of the proton from the enol to the Michael acceptor. It first has to be clarified whether this is a one- or a two-step process. If it is a two-step process, either the one with the C–C bond formed but the proton not transferred (**n5a**) or the one with the proton transferred but the C–C bond not yet formed (**n5b**). Neither of the two intermediates could be located as minima, as both of them fell back to **n4**. Having ruled out the possibility of a two-step process, the only possibility was to locate a transition state with a reasonable energy that could lead directly from **n4** to **n6**. In this transition state there should be a simultaneous formation of the C–C bond and transfer of the enol hydrogen to the Michael acceptor. For geometrical reasons, if both reactants are to be coordinated to the metal, the structure of such a transition state is highly tensioned and has therefore too high an energy for the reaction to advance unless at very high temperatures, which experimentally is not the case. Nevertheless, we tried to locate this transition state, but despite the necessary existence of at least one transition state between two minima, even if it has a very high energy, we could not locate it among the different reasonable geometries we tried. The impossibility of the direct or the two-step formation of the C–C bond does not completely rule out the possibility of an assisted transfer of the proton via a water molecule, for instance, present in trace levels. However, the necessary intervention of a fourth molecule in very low concentration makes the reaction rate slower, which means the neutral mechanism will be at least a slow one, if possible at all. The major contribution to the product will therefore not be due to this mechanism, despite the reasonable thermodynamics it exhibited (see Figure 6).

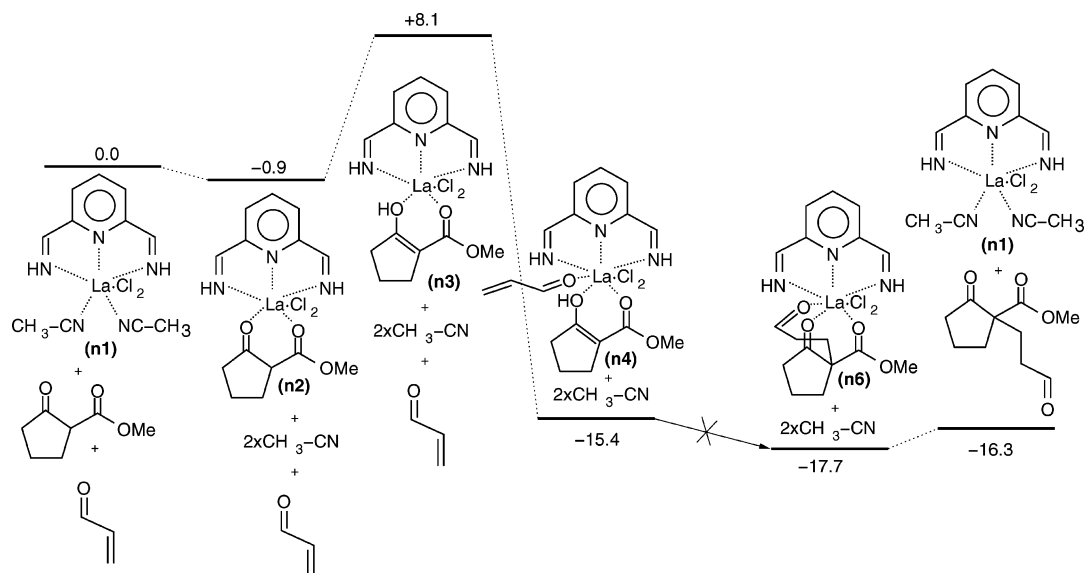


FIGURE 6. Reaction profile for the neutral pathway. Energies are in kcal/mol and relative to the reactants.

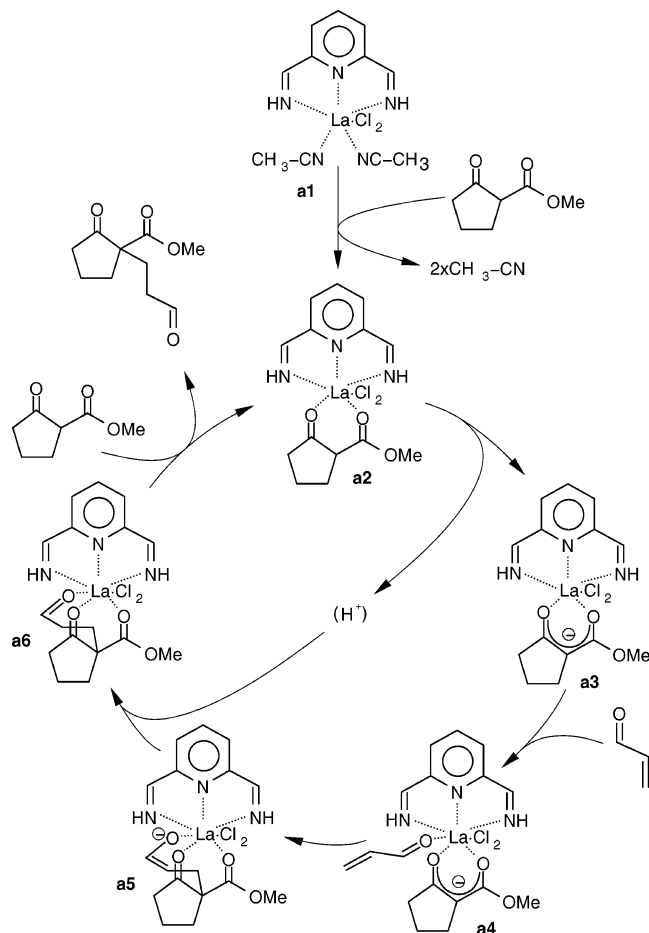


FIGURE 7. Catalytic cycle for the anionic pathway. Molecules **a1**, **a2**, and **a6** have a +1 charge, and the rest of them are neutral.

Anionic Mechanism. The presence of a base in the reaction medium, an excess of the chiral ligand, made us consider a second mechanism involving the dicarbonyl and enolate forms of the ketoester, hereafter being referred to as the anionic

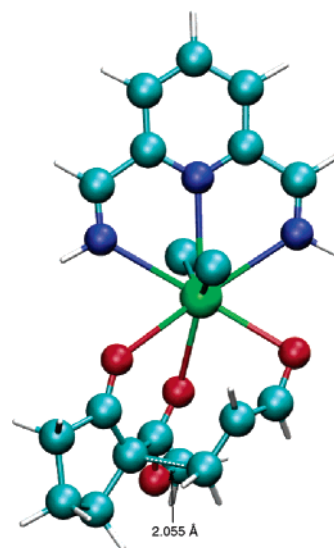


FIGURE 9. Transition state for step **a4** to **a5** in the anionic mechanism.

mechanism. This catalytic cycle and energy profile are shown in Figures 7 and 8. Different to the neutral case in this mechanism, only **a2** and **a6** are charged with a positive charge, whereas the rest of the intermediates are neutral due to the anionic charge in the ketoester moiety. The catalytic cycle for this anionic mechanism starts as in the neutral case by replacing two solvent molecules by the ketoester. The main difference comes next, when instead of turning the coordinated ketoester into the enol, its acidic proton is abstracted, turning the ketoester into the enolate form (**a3**), leaving the intermediate uncharged. The base responsible for the proton abstraction is probably the basic ligand excess in the first few cycles and the anionic product (**a5**) afterward. The profile in Figure 7 is computed according to this last case. The next step corresponds to the coordination of the second reactant, the Michael acceptor. Again, as in the neutral case, the deprotonation and coordination of the Michael donor can happen in any order but the result will in both cases be **a4**. The next step is the critical one, in which the C–C bond

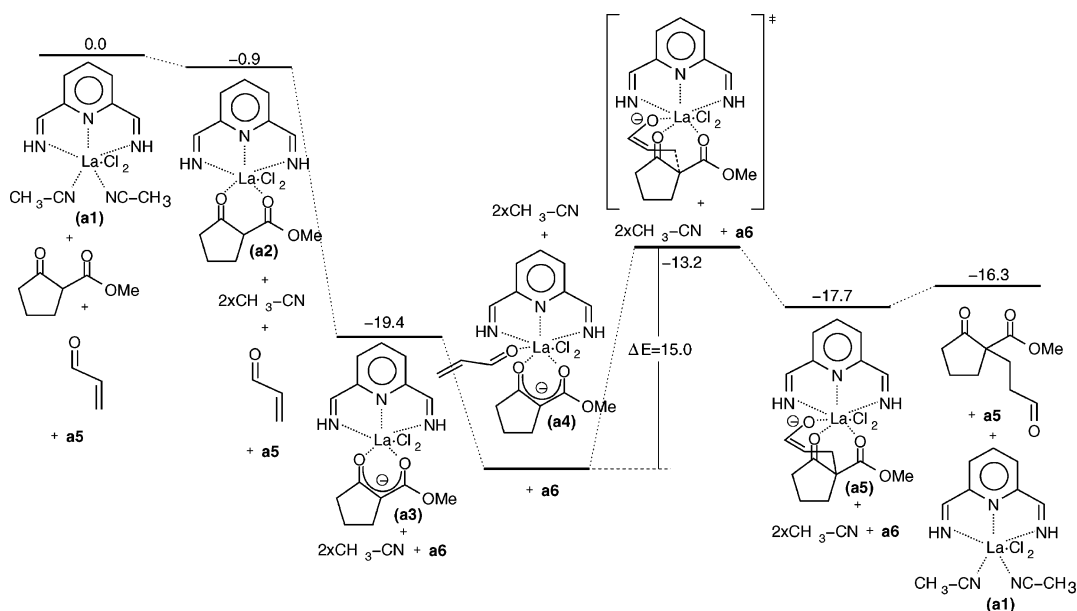


FIGURE 8. Reaction profile for the anionic pathway. Energies are in kcal/mol and relative to the reactants. The proton source for the protonation and sink for the deprotonation steps are the intermediates **a2** and **a5**, respectively.

is formed. In contrast to the neutral case, no proton must be transferred to the Michael acceptor, as the ketoester is in the enolate form and therefore lacking the proton. Furthermore, not only is the inexistent intermediate **n5a** in the neutral case stable now (**a5**), but it was also possible to connect **a4** to **a5** with a transition state. As only the C–C bond has to be formed, the geometry of this transition state, shown in Figure 9, is not especially tensioned. It is therefore expected that its energy will not be too high above that of **a4**, which is indeed the case, 15.6 kcal/mol. With the product almost formed, the next step corresponds to the protonation of **a5**. This protonation is carried out by another **a2** molecule starting another cycle (recall that **a5** deprotonated **a2** at the beginning of the cycle). This yields the final product coordinated to the lanthanum (**a6**), which can be easily replaced by a new ketoester molecule. The cycle is therefore ready to start again. Postulated intermediates **a2**, **a3**, and **a6** are in agreement with some of the observed species in the ESI mass spectrometry: **a2**, $m/z = 1000$ [(pybox)La(**1c**)-(OTf)₂]⁺; **a3**, $m/z = 850$ [(pybox)La(enolate-**1c**)OTf]⁺; **a6**, $m/z = 1070$ [(pybox)La(**8c**)(OTf)₂]⁺.

The knowledge of a possible and a forbidden pathway enables us to analyze the role of the metal in this reaction. One of the most obvious role of the metal is coordinating to both reactants and keeping them close to each other for long enough so that they can react. This alone should facilitate the reaction, and is required for the reaction being enantioselective. Furthermore, the metal, as an electron withdrawing center can activate the Michael acceptor. This activation is achieved by pulling the electrons in the π system close to the metal, as can be seen from the different O=CH–CH=CH₂ distances in the isolated molecule and the bound one (1.223, 1.475, 1.342, and 1.238 Å; 1.464 and 1.344 Å, respectively). This leaves the terminal methylene partially charged and eases the attack of a nucleophile. The two mechanisms studied above exhibit these two kinds of activation, so there must still be a difference that makes one of them possible and the other one forbidden. The key is again the electron-withdrawing character of the metal. Just as the coordination of the Michael acceptor to the metal lowers its electron density, so does the coordination of the nucleophile. Nevertheless, the activation of the nucleophile is achieved by increasing its electron density so that coordinating it to the metal effectively deactivates it, which explains the impossibility to proceed through the neutral pathway. Apart from merely deactivating the nucleophile, the lowering of the electron density also increases the acidity of the already acidic proton α to both carbonyls. This, in turn, eases the deprotonation of the reactant by both, the excess basic ligand and the charged intermediate **a5**, leaving a negative charge on the nucleophile and in effect activating it. It is this kind of activation that makes the difference between the neutral and anionic pathway and permits the reaction.

Conclusion

We have found that reactions of alkyl 2-oxocyclopentane dicarboxylates, **1**, with azodicarboxylates and butenone can be carried out with excellent chemical yields and ee's (up to 100%) using acetonitrile as solvent, europium, ytterbium triflates, and commercial-accessible (*S,S*)-ip-pybox as chiral ligand. We have observed that an excessive steric hindrance in the chiral ligand could be detrimental for high ee's, isopropyls giving better results than adamantyls as substituents in pybox. Moreover, the X-ray diffraction of two compounds permitted a safe assignment

of absolute configuration (*R*) for products of electrophilic amination. ESI-MS and NMR experiments were used to detect reaction intermediates. A simultaneous coordination of the lanthanide with the chiral ligand and the β -ketoester enolate is proposed as the key intermediate. Two different catalytic cycles have been studied through theoretical calculations. Finally, a mechanistic pathway has been proposed based on the cited intermediate. Moreover, understanding the mechanistic pathway provided the role of both the lanthanide center (increasing the acidity of the α proton of Michael donor and increasing the electrophilicity of the Michael acceptor) and the chiral ligand, acting not only in the generation of selectivity but also as a base.

Experimental Section

(*S,S*)-ip-pybox, **4a**, and ethyl 2-oxocyclopentanecarboxylate, **1a**, are commercially available, *t*-butyl 2-oxocyclopentanecarboxylate, **1b**,²⁴ was prepared according to described procedures, and 1-adamantyl 2-oxocyclopentanecarboxylate, **1c**, was prepared from a mixture of ketoester **1a**, 1-adamantanol, and zinc oxide (see Supporting Information). Zinc was activated by treatment with dilute HCl as described elsewhere.²⁵

Reactions between Ketoesters 1 and Electrophiles 2 and 7. General Method. A solution of Ln(OTf)₃ (0.017 mmol) and pybox **4** (0.023 mmol) in dichloromethane or acetonitrile (1.5 mL) was stirred overnight in the presence of 4 Å molecular sieves under inert atmosphere. The mixture was placed at the selected temperature. Then, the ketoester **1** (0.184 mmol) and the electrophile, **2** or **7**, (0.298 mmol) were sequentially added. The mixture was stirred for the time indicated in the tables (tlc monitoring), and the product was chromatographed through a silica gel column with hexanes–ethyl acetate as eluent.

tert-Butyl 2-oxo-1-[*N,N'*-bis(*tert*-butoxycarbonyl)hydrazino]cyclopentanecarboxylate, **3b.** Oil; IR (ATR) 3350, 2977, 2932, 1761, 1704, 1366, 1234, 1150, 1118 cm⁻¹; ¹H NMR (CDCl₃) δ 1.47 (s, 27H, *t*-Bu), 1.93–2.63 (complex absorption, 6H, CH₂), 6.50 (s, 1H, NH); ¹³C NMR (CDCl₃) δ 19.0, 28.3, 28.4, 28.5, 33.0, 38.0, 81.7, 83.0, 154.9, 155.6, 167.5, 208.0; ESI-MS m/z 437.1 (M+Na)⁺, 850.7 (2M+Na)⁺. Anal. calcd for C₂₀H₃₄N₂O₇: C, 57.95%; H, 8.27%; N, 6.76%. Found: C, 58.27%; H, 8.33%; N, 6.70%. [α]_D = +11.3° (*c* = 1.6, CH₂Cl₂).

The ee was determined in compound **5b**.

1-Adamantyl 2-oxo-1-[*N,N'*-bis(*tert*-butoxycarbonyl)hydrazino]cyclopentanecarboxylate, **3c.** Mp 120–120.5 °C; IR (ATR) 3337, 2976, 2910, 1758, 1711, 1363, 1232, 1150, 1048 cm⁻¹; ¹H NMR (CDCl₃) δ 1.41 (br s, 18H), 1.61 (br s, 6H), 1.84–2.62 (m, 14H), 6.44 (br s, 1H); ¹³C NMR (CDCl₃) δ 18.9, 28.4, 28.5, 31.2, 36.4, 41.4, 81.6, 82.8, 154.9, 155.5. Anal. calcd for C₂₆H₄₀N₂O₇: C, 63.39%; H, 8.18%; N, 5.69%. Found: C, 63.56%; H, 8.21%; N, 5.69%. [α]_D = +7.46° (*c* = 3.27, CH₂Cl₂) for 100% ee.

tert-Butyl (1*R*)-2-oxo-1-(3-oxobutyl)cyclopentanecarboxylate, **8b.** Oil; IR (ATR) 2975, 2932, 1745, 1710, 1368, 1253, 1140, 845 cm⁻¹; ¹H NMR (CDCl₃) δ 1.42 (s, 9H), 1.80–2.08 (complex absorption, 5H), 2.13 (s, 3H), 2.20–2.50 (complex absorption, 4H), 2.71 (ddd, *J* = 5.6, 9.8 and 17.7 Hz, 1H); ¹³C NMR (CDCl₃) δ 19.9, 27.4, 28.2, 30.3, 34.9, 38.3, 39.3, 59.8, 82.3, 171.0, 208.3, 215.5; [α]_D = +2.9° (*c* = 11.0, CH₂Cl₂; lit.^{14a} [α]_D = +8.7° (*c* = 0.41, CHCl₃) for 92% ee (*R*)).

Enantiomeric excess was determined by two different methods:

i. Integration of the different signals of methylenic protons (–CH₂–CO–CH₃, as ddd at δ 2.72 ppm) using the chiral shift

(24) Henderson, D.; Richardson K. A.; Taylor, R. J. K. *Synthesis* **1983**, 996.

(25) Hannaford, A. J.; Smith, P. W. G.; Tatchell, A. R. *Vogel's Textbook of Practical Organic Chemistry*, 5th ed; Furniss, B.S., Ed.; Longman: Singapore, 1989.

reagent $\text{Eu}(\text{hfc})_3$. Compound **8b** (10.7 mg, 0.0421 mmols) and $\text{Eu}(\text{hfc})_3$ (1.9 mg, 0.0016 mmols, 0.037 equiv) were dissolved in CDCl_3 (0.5 mL). ^1H RMN (250 MHz, CDCl_3) δ (ppm): $\delta_S = 2.9638$ ppm, $\delta_R = 2.9509$ ($\Delta(\Delta\delta)_{R,S} = 0.013$ ppm).

ii. Integration after addition of the chiral solvating agent (*R,R*)- α,α' -bis(trifluoromethyl)-9,10-anthracenedimethanol ((*R,R*)-ABTE).¹²

1-Adamantyl (1*R*)-2-oxo-1-(3-oxobutyl)cyclopentanecarboxylate, 8c. Mp 60.5–61.5 °C (racemic), oil (enantiomerically enriched); IR (ATR) 2971, 2913, 1747, 1710, 1191, 1155, 1049 cm^{-1} ; ^1H NMR (CDCl_3) δ 1.62 (br s, 6H), 1.80–2.02 (complex absorption, 5H), 2.03–2.18 (complex absorption, 12H), 2.20–2.50 (complex absorption, 4H), 2.73 (ddd, $J = 5.6, 9.8,$ and 17.7 Hz, 1H); ^{13}C NMR (CDCl_3) δ 19.8, 27.3, 30.1, 30.9, 31.0, 34.8, 36.2, 38.2, 39.1, 41.3, 45.5, 59.7, 82.2, 170.5, 208.2, 215.4. Anal. calcd for $\text{C}_{20}\text{H}_{28}\text{O}_4$: C, 72.26%; H, 8.49%. Found: C, 72.21%; H, 8.52%. $[\alpha]_D = +17.36^\circ$ ($c = 3.27, \text{CH}_2\text{Cl}_2$) for 80% ee (entry 4, Table 3).

Reactions of Elimination of *N-tert*-butoxycarbonyl group.

General method. Ytterbium triflate (9.9 mg, 0.016 mmol) was added to compounds **3a–c** (0.176 mmol) in dichloromethane (1 mL). The solution was stirred overnight, and the solution was chromatographed through silica gel with hexanes–ethyl acetate to afford compounds **5a–c**.

tert-Butyl 2-oxo-1-[*N'*-(*tert*-butoxycarbonyl)hydrazino]cyclopentanecarboxylate, 5b.

IR (ATR) 3398, 3321, 2978, 1751, 1720, 1243, 1148, 730 cm^{-1} ; ^1H NMR (CDCl_3) δ 1.46 (s, 18H) (two *t*-Bu), 2.05–2.56 (complex absorption, 6H) (CH_2 in cycle), 4.27 (s, 1H, NH–C-cycle), 6.48 (s, 1H, *NHCO*); ^{13}C NMR (CDCl_3) δ 19.7, 28.3, 28.6, 32.4, 37.7, 74.1, 80.7, 83.5, 156.6, 171.1, 211.1; ESI⁺-MS (m/z) 337.2 ($\text{M}+\text{Na}$)⁺; HRMS calcd for $\text{C}_{15}\text{H}_{26}\text{O}_5\text{N}_2$: 314.1842. Found: 314.1828.

Anal. calcd for $\text{C}_{15}\text{H}_{26}\text{O}_5\text{N}_2$: C, 57.31%; H, 8.34%; N, 8.91%. Found: C, 56.60%; H, 8.47%; N, 8.72%.

1-Adamantyl 2-oxo-1-[*N'*-(*tert*-butoxycarbonyl)hydrazino]cyclopentanecarboxylate, 5c. It was obtained as a white solid; mp 108–109 °C (racemic); IR (ATR) 3404, 3372, 2908, 2853, 1738, 1725, 1693, 1237, 1167, 1051 cm^{-1} ; ^1H NMR (CDCl_3) δ 1.41 (s, 9H), 1.62 (t, $J = 2.8$ Hz, 6H), 2.05–2.46 (m, 15 H), 4.23 (s, 1H), 6.46 (s, 1H); ^{13}C NMR (CDCl_3) δ 19.0, 28.0, 30.5, 31.8, 35.7, 37.0, 40.9, 73.5, 79.9, 82.9, 156.0, 170.1, 210.4. Anal. calcd for $\text{C}_{21}\text{H}_{32}\text{N}_2\text{O}_5$: C, 64.26%; H, 8.22%; N, 7.14%. Found: C, 64.24%; H, 8.22%; N, 7.16%.

Acknowledgment. We acknowledge financial support from “Ministerio de Educacion y Ciencia” of Spain (Projects BQU2002-04002, CTQ-2005-04968, BQU2003-05093, CTQ2005-09000-CO2-01, CTQ2006-01080) and “Generalitat de Catalunya” (Projects 2005SGR00305, 2005SGR00896).

Supporting Information Available: ESI-MS spectrum corresponding to experiments of Table 4. Full experimental details on the preparation of compounds **4b** and **1c**. ^1H and ^{13}C NMR and IR of **4b**, **1b**, **1c**, **3b**, **3c**, **5b**, **5c**, **8b**, and **8c**. ^1H NMR of **5b**+ $\text{Eu}(\text{hfc})_3$. ^1H NMR at variable temperature, DOSY and NOESY spectra of different mixtures of **4a**, $\text{La}(\text{OTf})_3$, and **1c**. HPLC chromatograms of **4b**, **3c**, **8b**, and **8c**. Tables of atom coordinates and absolute energies corresponding to the theoretical calculations. Complete data parameters of X-ray diffraction structures of compounds **3c** and **6**. This material is available free of charge via the Internet at <http://pubs.acs.org>.

JO0622678